Synthesis and Characterization of Zirconium and Iron Complexes Containing Substituted Indenyl Ligands: Evaluation of Steric and Electronic Parameters

Christopher A. Bradley, Samuel Flores-Torres, Emil Lobkovsky, Hector D. Abruña, and Paul J. Chirik*

Department of Chemistry and Chemical Biology, Baker Laboratory, Cornell University, Ithaca, New York 14853

Received June 14, 2004

Evaluation of the steric and electronic influence of a family of silyl- and alkyl-substituted indenyl ligands on zirconium and iron centers has been accomplished by a combination of X-ray diffraction, IR spectroscopy, solution NMR dynamics, and electrochemical measurements. Three tetrasubstituted, bis-indenyl zirconocene dichloride complexes have been characterized by X-ray diffraction and adopt a gauche ligand conformation such that the interactions between tertiary substituents on adjacent rings are minimized. Similar solid state conformations were also observed in two of the corresponding iron compounds. Evaluation of the electronic environment about each zirconium center was achieved by measurement of the CO stretching frequencies of the dicarbonyl derivatives. Simple inductive effects govern the electronic properties of each zirconocene where silyl groups are relatively electron withdrawing and alkyl groups electron donating. For the most hindered zirconocene dicarbonyl derivatives, population of three vibrationally distinct rotamers has been detected by IR spectroscopy. Independent assessment of these stereoelectronic parameters by variable-temperature NMR spectroscopy and electrochemistry with the analogous series of iron complexes provided the same relative ordering of the indenyl ligands.

Introduction

Substituted cyclopentadienyl and related indenyl anions occupy a prominent role in organometallic chemistry, serving as versatile ligands for main group elements, transition metals, and actinides.[1] Seemingly subtle changes in either cyclopentadienyl or indenyl ligand substitution can have profound consequences on chemical reactivity. For example, manipulation of alkyl and silyl groups on the ligand scaffold in group 4 metallocene-promoted olefin polymerization determines catalyst symmetry and therefore stereochemistry and physical properties of the resulting polyolefin.[2] While these effects are reasonably well understood for rigid *ansa*-metallocenes,[3] unbridged cyclopentadienyl and indenyl ligated zirconium precatalysts often display variable activities and levels of stereocontrol that are dependent on both activator[4] and ring substituents.[5]

Investigations in our laboratory focusing on the chemistry of low-valent group 4 metallocenes have demonstrated the importance of cyclopentadienyl and indenyl substituent effects. Both the steric and electronic influences imparted by cyclopentadienyl substituents govern the rate and outcome of alkane reductive elimination reactions. In some cases, stable zirconocene cyclometalated hydrides are obtained, while in another, N_2 coordination to form an activated, side-on bound N_2 complex results.[6] More recently we have demonstrated that the number of cyclopentadienyl methyl groups on a low-valent zirconocene dictates both the hapticity and reactivity of coordinated N_2. Whereas $[(\eta^5\text{-}C_5Me_5)_2Zr(\eta^1\text{-}N_2)]_2(\mu_2,\eta^1,\eta^1\text{-}N_2)$ contains weakly activated, end-on bound dinitrogen ligands that are easily displaced by H_2,[7] removal of one methyl group from each Cp* ring yields a strongly activated zirconocene dinitrogen complex that promotes the hydrogenation of N_2 to ammonia with mild thermolysis.[8] We have also discovered profound reactivity differences on replacing cyclopentadienyl with their indenyl counterparts. Instead of cyclometalation or N_2 activation, reductive elimination of isobutane from $(\eta^5\text{-}C_9H_5\text{-}1,3\text{-}(SiMe_3)_2)_2Zr(CH_2CHMe_2)H$ yields a zirconium sandwich complex that provides convenient access to an isolable Zr(II) equivalent. This unusual "zirconocene" promotes C−H activation under mild conditions, readily coordinates alkynes, and undergoes haptotropic rearrangement to its η^6, η^5 isomer upon addition of THF.[9]

Prompted by these striking effects on chemical reactivity, we sought to methodically characterize the stereoelectronic properties of a class of 1,2-disubstituted

(1) For leading reviews on metallocene chemistry see: *Metallocenes: Synthesis, Reactivity and Applications*; Togni, A., Halterman, R. L., Eds.; Wiley-VCH: Weinheim, 1998.
(2) Coates, G. W. *Chem. Rev.* **2000**, *100*, 1223.
(3) Ewen, J. A. *Sci. Am.* **1997**, *276*, 86.
(4) Chen, M.-C.; Roberts, J. A. S.; Marks, T. J. *J. Am. Chem. Soc.* **2004**, *126*, 4605.
(5) Möhring, P. C.; Coville, N. J. *J. Organomet. Chem.* **1994**, *479*, 1.
(6) Pool, J. A.; Lobkovsky, E.; Chirik, P. J. *J. Am. Chem. Soc.* **2003**, *125*, 2241.
(7) Manriquez, J. M.; Bercaw, J. E. *J. Am. Chem. Soc.* **1974**, *96*, 6229.
(8) Pool, J. A.; Lobkovsky, E.; Chirik, P. J. *Nature* **2004**, *427*, 527.
(9) Bradley, C. A.; Lobkovsky, E.; Chirik, P. J. *J. Am. Chem. Soc.* **2003**, *125*, 8110.

10.1021/om0495675 CCC: $27.50
Publication on Web 09/29/2004

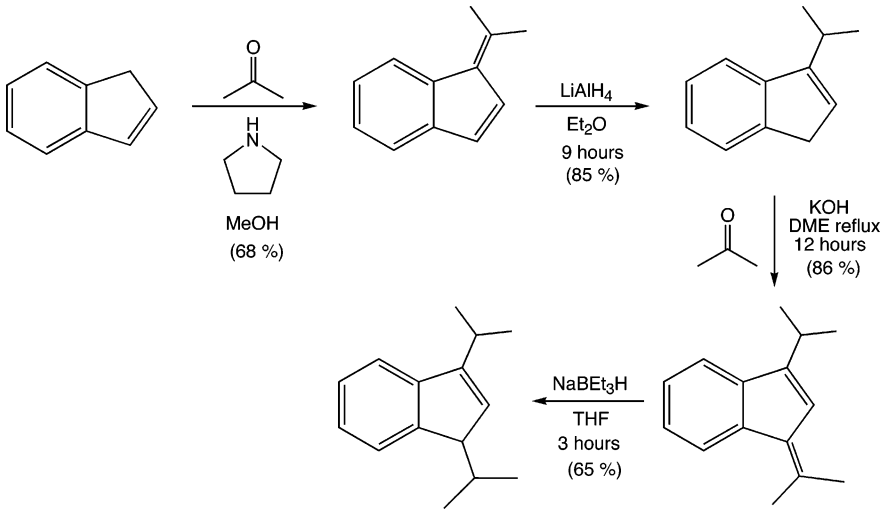

Figure 1. Synthesis of 1,3-diisopropylindene.

indenyl ligands with sterically demanding silyl and alkyl substituents. A similar, comprehensive study on the electronic properties of cyclopentadienyl ligands in the context of elucidating the "*ansa*-effect" in group 4 metallocene chemistry has recently appeared.[10] The goal of this study is to gain a fundamental understanding of the features of assorted indenyl ligands such that "zirconocenes" with specifically tailored properties and reactivity patterns can be synthesized. X-ray diffraction, infrared spectroscopy, and dynamic NMR studies provided insight into the steric influence of the family of ligands, while cyclic voltammetry and infrared spectroscopy were used as a measure of ligand electronics.

Results and Discussion

Synthesis of Bis-indenyl Zirconocene Dichloride Complexes. Our studies began with the synthesis of a variety of tetrasubstituted bis-indenyl zirconium dichloride complexes where the substituents on the indenyl ligands were systematically varied. The requisite 1,3-disilyl-substituted indenide anions were prepared in a straightforward manner by treatment of the appropriate lithium indenide with various silyl chlorides.[11] Complete experimental details for each synthesis can be found in the Supporting Information. We also targeted preparation of a 1,3-dialkyl-substituted indene. Reports of the synthesis of the 1,3-diisopropylindenide anion and its coordination chemistry have appeared previously,[12,13] although to our knowledge a detailed synthesis of the ligand has not been described. Our preparation commenced with the condensation of acetone with commercially available indene in the presence of stoichiometric pyrollidine base to cleanly afford 8,8-dimethylbenzofulvene in 68% yield (Figure 1).[14] Subsequent reduction with $LiAlH_4$ followed by careful hydrolysis provided 3-isopropylindene. In our hands, a second condensation with acetone in the presence of KOH furnished 3-isopropyl-8,8-dimethylbenzofulvene. This result contrasts a previous report where an isopropylidene-linked bis-indene was claimed from a similar procedure.[15] The synthesis of the desired 1,3-diisopropylindene was completed by reduction of 3-isopropyl-8,8-dimethylbenzofulvene with $NaBEt_3H$. Attempts to reduce the fulvene with $LiAlH_4$ yielded a mixture of products.

With a range of indenyl ligands in hand, homoleptic bis-indenyl zirconocene dichlorides were prepared in a straightforward manner by reacting 2 equiv of the appropriate indenide anion with $ZrCl_4$ in diethyl ether (eq 1). Each of the compounds prepared is shown in Figure 2 along with a shorthand designation and isolated yield. It should be noted that the synthesis of **4-Cl$_2$** yielded a near equimolar mixture of *rac* and *meso* isomers that were not separated.

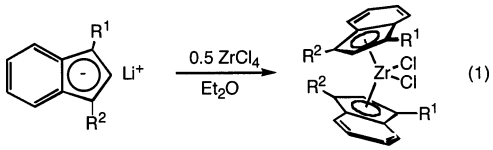

(1)

The synthesis of "mixed ring" bis-indenyl zirconocene dichlorides was also achieved. Preparation of the requisite mono-indenyl, piano stool complex, $[(\eta^5\text{-}C_9H_5\text{-}1,3\text{-}(SiMe_3)_2)ZrCl_3\cdot(Et_2O)_2LiCl_x]_n$, was accomplished by addition of 1 equiv of $Li[C_9H_5\text{-}1,3\text{-}(SiMe_3)_2]$ to $ZrCl_4$ in diethyl ether (eq 2). Both ^1H and ^{13}C NMR spectroscopy confirmed the presence of 2 equiv of diethyl ether. Satisfactory elemental analyses were not obtained due to coordination of variable amounts of LiCl from sample to sample. While isolated material was effective for subsequent transformations, we discovered that in situ generation of the piano stool compound was the most convenient and reproducible method for the synthesis of the desired mixed ring bis-indenyl zirconocene dichloride complexes. In this manner, the tetrasubstituted compounds **6-Cl$_2$** and **7-Cl$_2$** were isolated in modest yields (Figure 2). This procedure was also extended to include the synthesis of trisubstituted complexes such

(10) Zachmanoglou, C. E.; Bridgewater, B. M.; Parkin, G. E.; Brandow, C. G.; Bercaw, J. E.; Jardine, C. N.; Lyall, M.; Green, J. C.; Kiester, J. B. *J. Am. Chem. Soc.* **2002**, *124*, 9525.
(11) Brady, E. D.; Overby, J. S.; Meredith, M. B.; Mussman, A. B.; Cohn, M. A.; Hanusa, T. P.; Yee, G. T.; Pink, M. *J. Am. Chem. Soc.* **2002**, *124*, 9556.
(12) Overby, J. S.; Hanusa, T. P.; Sellers, S. P.; Yee, G. T. *Organometallics* **1999**, *18*, 3561.
(13) Overby, J. S.; Hanusa, T. P. *Organometallics* **1996**, *16*, 2212.
(14) Stone, K. J.; Little, R. D. *J. Org. Chem.* **1984**, *49*, 1849.
(15) Nifant'ev, I. E.; Ivchenko, P. V.; Kuz'ina, L.; Luzikov, Y. N.; Sitnikov, A. A.; Sizan, O. E. *Synthesis* **1997**, 469.

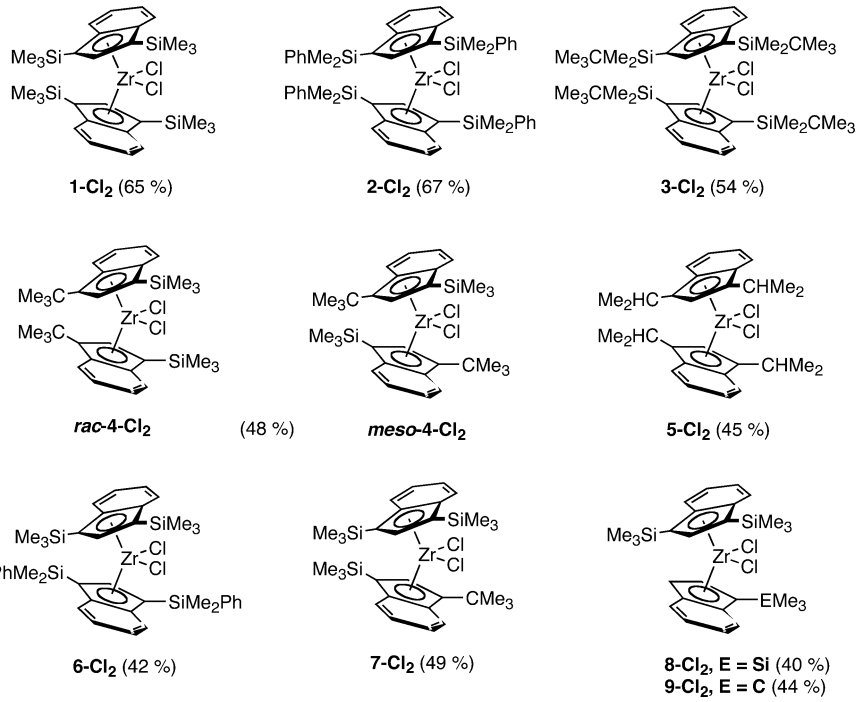

Figure 2. Labeling scheme and isolated yields of bis-indenyl zirconocene dichlorides.

as **8-Cl$_2$** and **9-Cl$_2$** (Figure 2). All of the bis-indenyl zirconocene dichloride complexes can be easily isolated as bright yellow, slightly air-sensitive crystalline solids in multigram quantities.

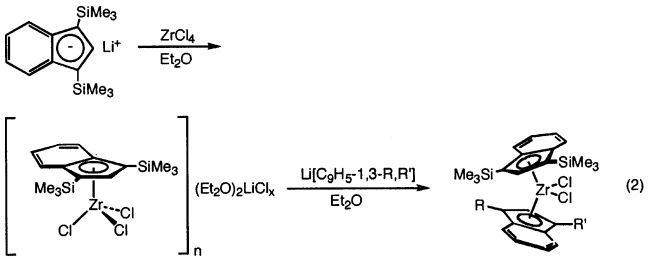

Each of the dichloride complexes was characterized by ^{1}H and ^{13}C NMR spectroscopy, elemental analysis, and in many cases, single-crystal X-ray diffraction. For **1-Cl$_2$**, **2-Cl$_2$**, **3-Cl$_2$**, and **5-Cl$_2$**, ^{1}H NMR spectra in benzene-d_6 display spectral features diagnostic of C_{2v} symmetric bent zirconocene derivatives. For example, the ^{1}H NMR spectrum of **1-Cl$_2$** exhibits one [SiMe$_3$] resonance, one cyclopentadienyl resonance, and two indenyl resonances, consistent with rapidly rotating indenyl ligands. This dynamic behavior was observed even at temperatures as low as −80 °C in toluene-d_8. The lower symmetry complexes such as **6-Cl$_2$**, **7-Cl$_2$**, **8-Cl$_2$**, and **9-Cl$_2$** exhibit the expected number of ^{1}H and ^{13}C resonances, the details of which can be found in the Experimental Section and Supporting Information.

The X-ray crystal structures of **1-Cl$_2$**, **2-Cl$_2$**, **7-Cl$_2$**, and **9-Cl$_2$** are shown in Figures 3−6. Crystals of **1-Cl$_2$** contain two independent, enantiomeric molecules in the asymmetric unit that differ slightly by the orientation of one of the indenyl rings. The two bulky rings are rotated in a perpendicular gauche-type arrangement to avoid steric interactions between the [SiMe$_3$] substituents. Similar conformations are observed for **2-Cl$_2$** and **7-Cl$_2$**. These metallocenes can be classified as class IV structures,[10] where the five-membered rings of the indenyl ligands are essentially eclipsed and four carbon atoms from each ring lie over the $ZrCl_2$ fragment. The most hindered example crystallographically characterized, **2-Cl$_2$**, has one silyl phenyl substituent oriented above an indenyl ring with the other directed away from the metallocene wedge. In contrast to tetrasubstituted zirconocenes, the indenyl ligands in the trisubstituted zirconocene dichloride, **9-Cl$_2$**, become more eclipsed due to the removal of one of the large *tertiary* silyl or alkyl substituents. In this case the structure can be categorized as a class III zirconocene,[10] where the five-membered rings stagger and there are three carbons over the $ZrCl_2$ portion of the molecule. The observed bond lengths in **1-Cl$_2$**, **2-Cl$_2$**, **7-Cl$_2$**, and **9-Cl$_2$** are typical for group 4 bent metallocene derivatives[1] and can found in the Supporting Information.

A more quantitative comparison of the structural parameters for each of the crystallographically characterized zirconocene dichlorides is presented in Tables 1 and 2. Using the methods originally described by Faller and Crabtree[16] and later expanded by Veiros,[17] the hapticity and relative orientation of the indenyl ligands can be defined (Table 1). The parameters for (η^5-C_9H_7)$_2$-$ZrCl_2$[18] and (η^5-C_9Me_7)$_2$$ZrCl_2$[19] are also included for comparison. The slip distortion (ΔM−C) and the fold angle (Ω) are used as a measure of the hapticity of the indenyl ligands. The first quantity (ΔM−C) is defined as the difference between the average distance from the metal center to the carbon atoms shared by the five- and six-membered rings (C(4) and C(9), Table 1) and

(16) Faller, J. W.; Crabtree, R. H.; Habib, A. *Organometallics* **1985**, *4*, 929.

(17) (a) Calhorda, M. J.; Felix, V.; Veiros, L. *Coord. Chem. Rev.* **2002**, *230*, 49. (b) Parkin has also updated these parameters: Trnka, T. M.; Bonanno, J. B.; Bridgewater, B. M.; Parkin, G. *Organometallics* **2001**, *20*, 3255.

(18) Repo, T.; Klinga, M.; Mutikainen, L.; Su, Y.; Leskela, M.; Polamo, M. *Acta Chem. Scand.* **1996**, *50*, 1116.

(19) O'Hare, D.; Murphy, V.; Diamond, G.; Arnold, P.; Mountford, P. *Organometallics* **1994**, *13*, 4689.

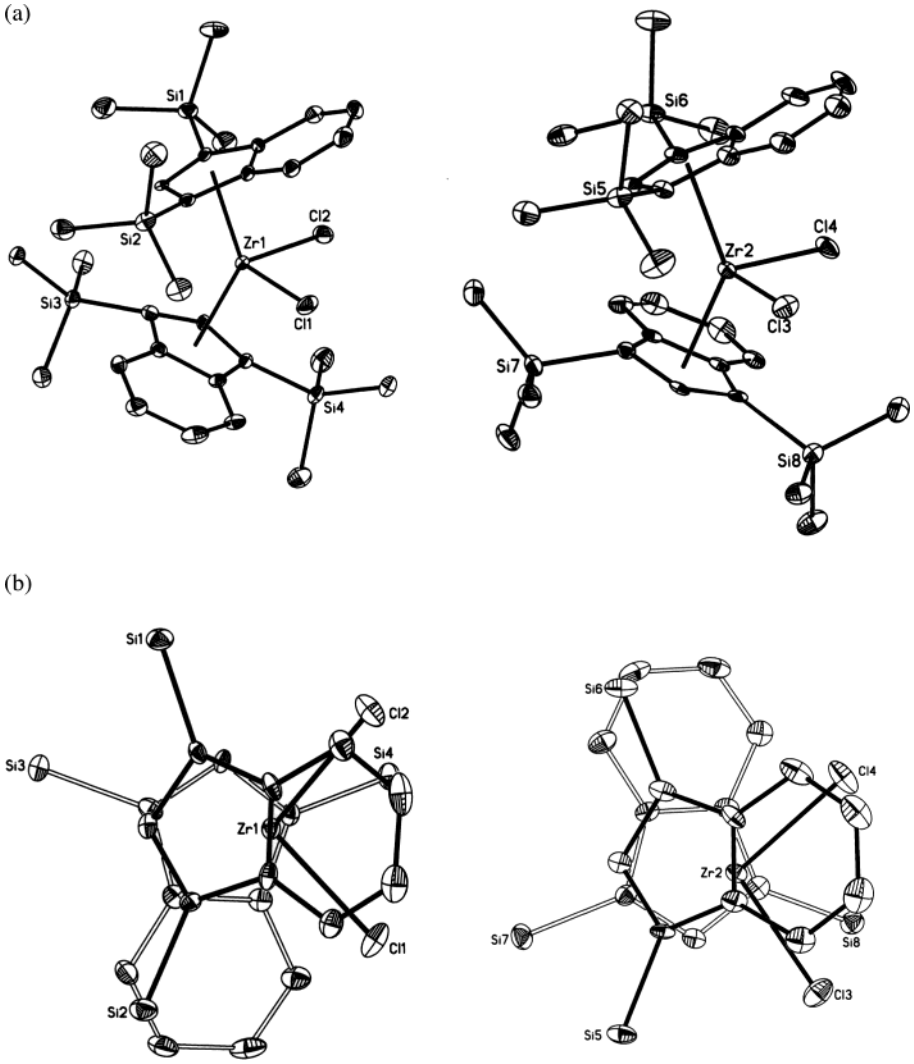

Figure 3. (a) Molecular structure of **1-Cl$_2$** with 30% probability ellipsoids. Hydrogen atoms are omitted for clarity. (b) Top view of the molecule with hydrogen atoms and silyl methyl groups omitted for clarity.

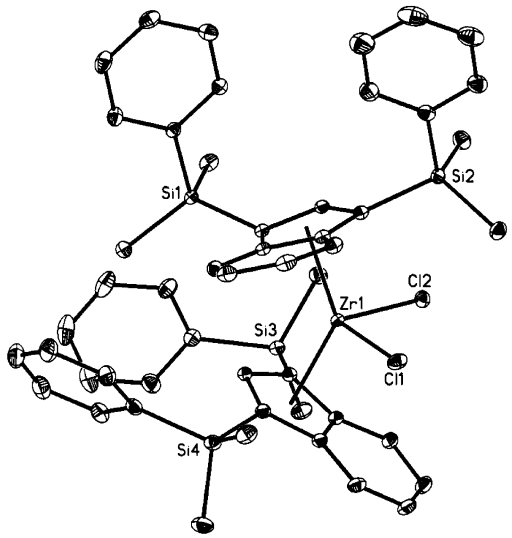

Figure 4. Molecular structure of **2-Cl$_2$** with 30% probability ellipsoids. Hydrogen atoms are omitted for clarity.

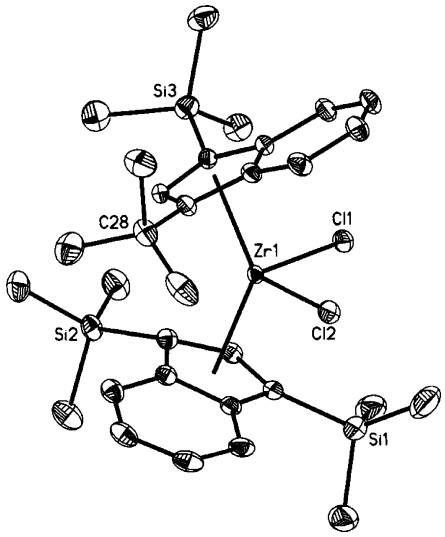

Figure 5. Molecular structure of **7-Cl$_2$** with 30% probability ellipsoids. Hydrogen atoms are omitted for clarity.

the adjacent carbon atoms unique to the five-membered ring (C(1), C(2), and C(3), Table 1). Typically metallocenes with slip distortions less than 0.30 Å are considered to have η^5 indenyl ligands.[16] The fold angle (Ω) is defined as the angle between the planes formed by the carbons unique to the five-membered ring (C(1)−C(2)−C(3)) and C(1)−C(3)−C(4)−C(9) (Table 1). Values of Ω less than 8° are usually associated with η^5 coordination.

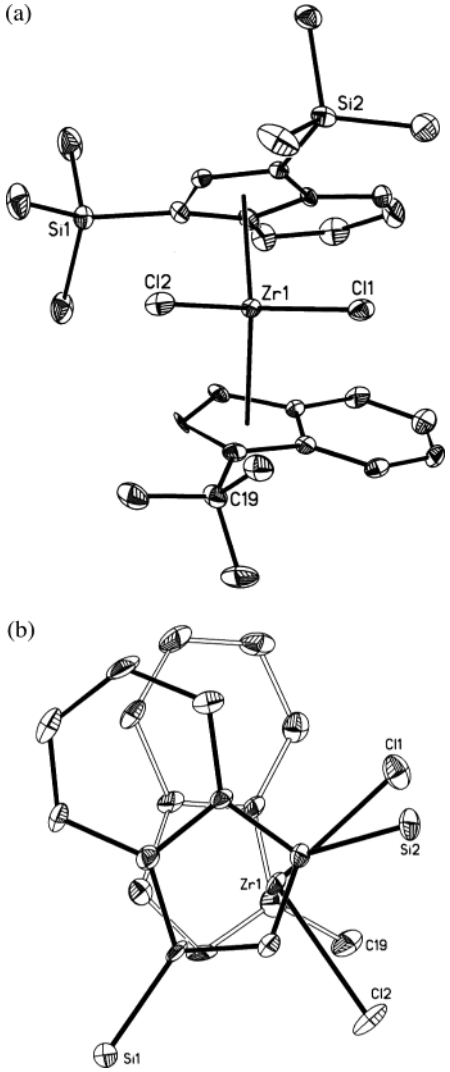

Figure 6. (a) Molecular structure of **9-Cl$_2$** with 30% probability ellipsoids. Hydrogen atoms are omitted for clarity. (b) Top view of the molecule with hydrogen atoms and silyl and *tert*-butyl substituents omitted for clarity.

Table 1. Structural Data for Bis-indenyl Zirconocene Dichloride and Dicarbonyl Complexes

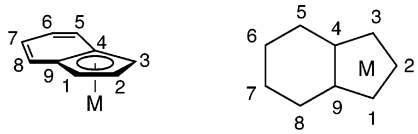

compound	slip distortion ΔM−C (Å)	fold angle Ω (deg)	rotational angle (deg)
1-Cl$_2$	0.121(6), 0.126(4)	3.3(2), 5.1(2)	89.7(5)
	0.106(5), 0.119(4)	2.994), 3.7(2)	95.3(5)
2-Cl$_2$	0.110(2), 0.098(2)	4.4(2), 4.5(2)	85.3(2)
7-Cl$_2$	0.149(3), 0.104(3)	5.2(3), 3.7(2)	79.8(2)
9-Cl$_2$	0.071(6), 0.098(6)	3.5(5), 4.2(4)	120.9(4)
1-(CO)$_2$	0.130(4), 0.114(3)	4.2(2), 3.6(2)	86.6(3)
3-(CO)$_2$	0.057(8), 0.022(8)	0.6(6), 0.5(6)	12.0(5)
(η^5-C$_9$H$_7$)$_2$ZrCl$_2$	0.115(6), 0.112(5)	5.2(4), 6.2(5)	36.3(5)
(η^5-C$_9$Me$_7$)$_2$ZrCl$_2$	0.039(4), 0.041(4)	5.9(4), 6.4(3)	88.7(4)

The range of the slip distortions, 0.071−0.149 Å, and fold angles, 2.9−5.2°, are consistent with η^5 hapticity for all of the indenyl ligands in the dichloride complexes crystallographically characterized in this study.

Table 2. Calculated Geometrical Data for Bis-indenyl Zirconocene Dichloride, Dicarbonyl Complexes, and Selected Cyclopentadienyl Derivatives

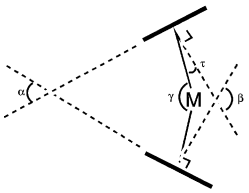

α = interplanar-ring angle

β = Cp$_{norm}$-Cp$_{norm}$; α +β =180°

γ = Cp$_{cent}$-M-Cp$_{cent}$

τ = tilt angle, 0.5(γ - β)

compound	α (deg)	β (deg)	γ (deg)	τ (deg)
1-Cl$_2$	47.7	132.3	135.9	1.8
	47.9	132.1	135.9	1.9
2-Cl$_2$	48.5	131.5	135.3	1.9
7-Cl$_2$	44.7	135.3	137.6	1.2
9-Cl$_2$	50.6	129.4	133.3	2.0
1-(CO)$_2$	33.9	146.1	151.7	2.8
3-(CO)$_2$	27.2	152.8	150.1	−1.5
Cp$_2$ZrCl$_2$[a]	53.5	126	129	1.4
Cp′$_2$ZrCl$_2$[a]	54	126	128	1.0
Cp$^t_2$ZrCl$_2$[a]	59	121	129	4.0
Cp″$_2$ZrCl$_2$[a]	51	129	130	1.0
Cp$^{tt}_2$ZrCl$_2$[a]	41	121	128	4.3
Cp*$_2$ZrCl$_2$[a]	43.7	136	130	2.7
(η^5-C$_9$H$_7$)$_2$ZrCl$_2$	59.3	121	128	3.8
(η^5-C$_9$Me$_7$)$_2$ZrCl$_2$	41	139	138	−0.4

[a] Data taken from ref 10. [b] Abbreviations used: Cp = η^5-C$_5$H$_5$, Cp′ = η^5-C$_5$H$_4$-SiMe$_3$, Cp^t = η^5-C$_5$H$_4$-CMe$_3$, Cp″ = η^5-C$_5$H$_3$-1,3-(SiMe$_3$)$_2$, Cp^{tt} = η^5-C$_5$H$_3$-1,3-(CMe$_3$)$_2$, Cp* = η^5-C$_5$Me$_5$.

The conformational preference of the indenyl ligands in the dichloride complexes can be described by the rotational angle (RA).[17] This quantity is the dihedral angle between the two planes of the indenyl defined by the metal−C(2) and the midpoint of the C(4)−C(9) carbons. A rotational angle of 0° corresponds to an eclipsed conformation, whereas a value of 180° indicates staggered indenyl ligands. It is important to note that for bent metallocenes such as those reported in this study the value of RA is also a measure of the angle between the rings. The data contained in Table 1 demonstrate the structural similarity of the tetrasubstituted bis-indenyl zirconocene dichloride complexes. For **1-Cl$_2$**, **2-Cl$_2$**, and **7-Cl$_2$**, rotational angles near 90° are observed, indicative of an essentially gauche arrangement of the indenyl ligands. Similar observations have been made for analogous chromium complexes[11] as well as in sterically hindered bis-indenyl iron and cobalt compounds.[20] The gauche conformation maximizes the distance between the sterically demanding substituents on adjacent indenyl rings. In contrast, **9-Cl$_2$** has a rotational angle of approximately 120°, demonstrating that rotational preference of each complex is dictated by the large, isotropic silyl or alkyl substituents. In all examples, crystal packing effects may also influence some of the observed rotational angles.

The angular parameters, α, β, γ, and τ, typically defined for bent bis-cyclopentadienyl complexes[10] have also been computed (Table 2). Values for several Cp compounds are also presented in Table 2 for comparison. The angular parameters for the tetrasubstituted compounds **1-Cl$_2$**, **2-Cl$_2$**, and **7-Cl$_2$** are similar, indicating

(20) Calhorda, M. J.; Veiros, L. F. *J. Organomet. Chem.* **2001**, *635*, 197.

little variation in geometry as a function of tertiary substituent. As is known in cyclopentadienyl chemistry,[10] the large substituents on the indenyl rings orient to avoid steric interactions in the narrow portion of the bent metallocene, producing a more linear arrangement of the rings. The values of α and β for these molecules are similar to those observed for $Cp^*_2ZrCl_2$ and $Cp^{Me4Et}_2ZrCl_2$,[10] suggesting that disubstitution on an indenyl ligand with tertiary silyl groups produces a ligand of similar steric disposition to a peralkylated cyclopentadiene. Deviation from this trend is observed for **9-Cl$_2$**, where replacement of one large substituent with a hydrogen atom results in decreased values of β and γ.

Evaluation of the Electronic Influence of the Indenyl Ligands. Having examined the structural features of several zirconocene dichlorides, a quantitative comparison of the electronic properties imparted by each substituted indenyl ligand was desired. Previous work with bis-cyclopentadienyl zirconium complexes has established that carbonyl stretching frequencies of $(CpR_n)_2Zr(CO)_2$ derivatives are a reliable measure of relative ligand electronics.[10] Preparation of the requisite bis-indenyl zirconium dicarbonyl complexes was accomplished by reduction of the corresponding dichloride with magnesium under an atmosphere of CO (eq 3). Each zirconocene dicarbonyl complex was isolated as a green, microcrystalline solid in moderate yield.

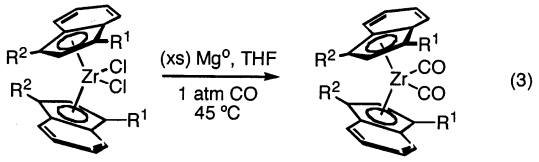

(3)

The homoleptic zirconocene dicarbonyl complexes **1-(CO)$_2$**, **2-(CO)**, **3-(CO)$_2$**, and **5-(CO)$_2$** display the expected number of ^{1}H and ^{13}C NMR resonances for C_{2v} symmetric molecules with rapidly rotating indenyl rings. This behavior is preserved even upon cooling to −80 °C. As observed for **4-Cl$_2$**, a near equimolar mixture of *rac* and *meso* isomers of **4-(CO)$_2$** was also isolated. This synthetic procedure was extended to include the "mixed ring" derivatives **7-(CO)$_2$**, **8-(CO)$_2$**, and **9-(CO)$_2$**. The solid state structure of **1-(CO)$_2$** has been communicated,[9] and the indenyl ligands adopt a conformation similar to that observed for **1-Cl$_2$**. As Figure 7 and the parameters in Tables 1 and 2 illustrate, the molecule adopts a gauche arrangement with a rotational angle of 86.6(3)°. Comparing the structures of **1-Cl$_2$** and **1-(CO)$_2$** demonstrates a contraction of α with concomitant expansion of β upon substitution of chloride for carbon monoxide. Such an effect is consistent with the metallocene becoming more linear as the steric congestion in the wedge is reduced. This behavior has also been noted upon replacement of chloride with hydride ligands.[21]

The zirconocene dicarbonyl complex containing large *tert*-butyldimethylsilyl substitutents, **3-(CO)$_2$**, was also characterized by X-ray diffraction. The solid state structure is shown in Figure 8 and exhibits a somewhat unexpected ligand conformation. The silyl groups are

(21) Chirik, P. J.; Day, M. W.; Bercaw, J. E. *Organometallics* **1999**, *18*, 1873.

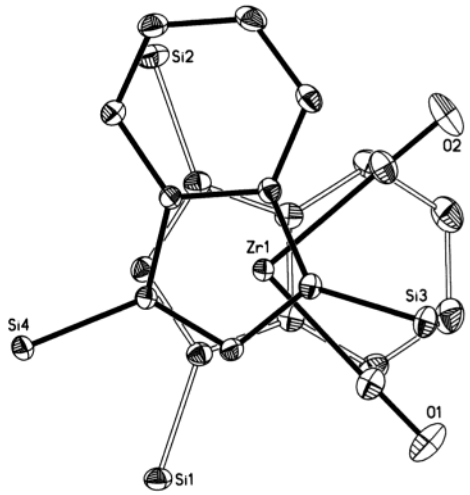

Figure 7. Top view of **1-(CO)$_2$**[9] with 30% probability ellipsoids. Hydrogen atoms and silyl methyl groups are omitted for clarity.

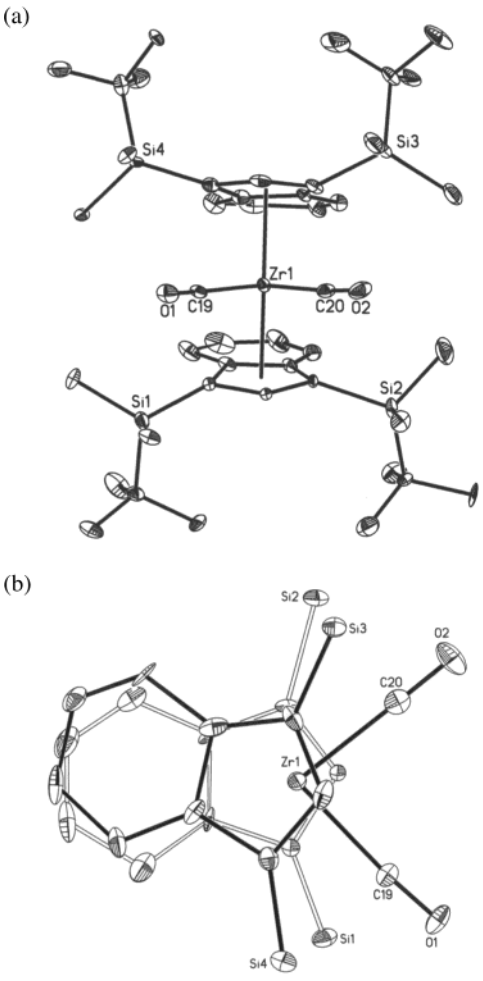

Figure 8. (a) Molecular structure of **3-(CO)$_2$** with 30% probability ellipsoids. Hydrogen atoms are omitted for clarity. (b) Top view with hydrogen atoms and silyl substituents omitted for clarity.

rotated such that the *tert*-butyl substituents are oriented toward the most open regions of the zirconocene, above and below the planes of their respective indenyl ligands. This conformation places the silyl methyl groups toward the interior of the molecule. The indenyl ligands are essentially eclipsed, with a rotational angle of only

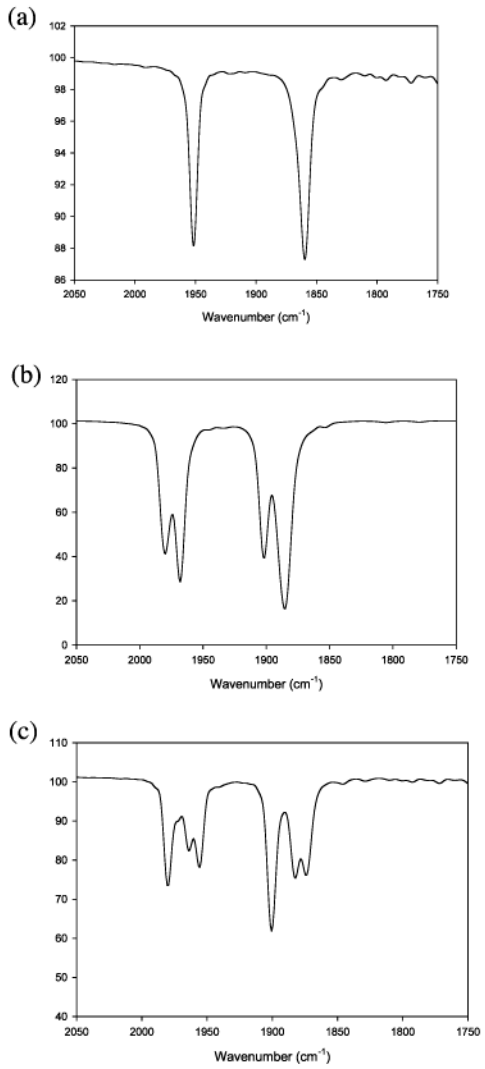

Figure 9. Infrared spectra of (a) **5-(CO)$_2$**, (b) **8-(CO)$_2$**, and (c) **1-(CO)$_2$**.

12.0(5)° (Table 1). In this orientation, all four silyl substituents avoid narrow portions of the metallocene and unfavorable transannular interactions with the benzo fragments of the indenes. This structure also produces a more linear zirconocene with values of α and β equal to 27.2 and 152.8°, respectively, as compared to 33.9 and 146.1° in **1-(CO)$_2$**, where the indenyl ligands adopt the more familiar gauche arrangement (Table 2). A similar eclipsed indenyl conformation is observed for (η^5-C_9H_7)$_2$Zr(CO)$_2$,[22] although in this case the two rings are oriented approximately 90° from the metallocene wedge whereas in **3-(CO)$_2$** the benzo rings are anti, approximately 180°, from the Zr(CO)$_2$ fragment.

The electronic environment imparted by each indenyl ligand was assessed by infrared spectroscopy. Representative spectra are shown in Figure 9, and the carbonyl stretching frequencies are compiled in Table 3. As typically observed for idealized C_{2v} symmetric bent zirconocene dicarbonyls, **5-(CO)$_2$** exhibits two intense CO bands centered at 1952 and 1859 cm^{-1}, corresponding to a symmetric and asymmetric stretch, respectively (Figure 9a). Comparing the average value of 1905.5 cm^{-1} to the value of 1915.5 cm^{-1} reported for (η^5-C_5H_3-1,3-(CHMe$_2$)$_2$)$_2$Zr(CO)$_2$ suggests that, in this case, the indenyl ligand is more electron donating than the corresponding cyclopentadiene.[10] In fact, the electronic environment of **5-(CO)$_2$** most closely resembles that of a tetrasubstituted cyclopentadiene such as (η^5-C_5Me_4H)$_2$-Zr(CO)$_2$, which has an average carbonyl stretching frequency of 1904.5 cm^{-1} in pentane solution.[10]

Table 3. Carbonyl Stretching Frequencies of Bis-indenyl Zirconium Dicarbonyl Complexes Recorded in Pentane

compound	ν(CO)$_{sym}$	ν(CO)$_{sym}$	ν(CO)$_{sym}$	ν(CO)$_{asym}$	ν(CO)$_{asym}$	ν(CO)$_{asym}$
1-(CO)$_2$	*1980*[a]	1964	1956	*1901*	1882	1874
2-(CO)$_2$	*1982*	1965	1957	*1902*	1883	1877
3-(CO)$_2$	1976	*1956*		1895	*1874*	
4-(CO)$_2$	1974	1951		1893	1863	
5-(CO)$_2$	1952			1859		
7-(CO)$_2$	1976	1956		1895	1874	
8-(CO)$_2$	1980	*1968*		1902	*1885*	
9-(CO)$_2$	1977	*1965*		1896	*1880*	

[a] Frequencies denoted in italics indicate the major isomer.

The infrared spectra of **7-(CO)$_2$**, **8-(CO)$_2$**, and **9-(CO)$_2$** contained *four* carbonyl bands. For **7-(CO)$_2$** the bands are approximately of equal intensity, whereas for **8-(CO)$_2$** and **9-(CO)$_2$**, a set of major and minor bands are observed (Table 3, Figure 9b). The zirconocene dicarbonyl complexes with larger indenyl ligands, **1-(CO)$_2$** and **2-(CO)$_2$**, exhibit a total of *six* carbonyl stretches. Similar observations were made in the solid state (KBr); however the resolution of the peaks is significantly reduced (Supporting Information). Despite the difference in the time scale of the IR experiment and the rotation of cyclopententadienyl ligands, to our knowledge this is the first observation of different rotamers of group 4 metallocene dicarbonyl complexes by IR spectroscopy.[23]

The spectrum of **1-(CO)$_2$** in pentane solution exhibits two major bands centered at 1980 and 1901 cm^{-1}, as well as four smaller peaks of approximately equal intensity (Figure 9c). To rule out the possibility that the additional bands were due to impurities, the single crystals used for both elemental analysis and X-ray diffraction[9] were examined by infrared spectroscopy and produced identical spectra. Furthermore, the relative intensities of the peaks were consistent from sample to sample, also arguing against impurities. The additional carbonyl bands arise from population of three different rotamers that have measurably different vibrational spectra (Figure 10).[23] Observation of different rotamers in solution complements Waymouth's recent report on the application of on-resonance spin−lattice relaxation in the rotating frame to measure the rate of rotation in several aryl-substituted bis-indenyl zirconocenes.[24]

Starting with the gauche arrangement observed in the solid state structure of **1-(CO)$_2$**, rotamers resulting from 90° rotation of one indenyl ligand are considered for simplicity, although other intermediate rotations are certainly plausible. Regardless of rotamer structure, it

(22) Rausch, M. D.; Moriarity, K. J.; Atwood, J. L.; Hunter, W. E.; Samuel, E. *J. Organomet. Chem.* **1987**, *327*, 39.

(23) For examples in iron and chromium chemistry see: (a) Mackie, S. C.; Baird, M. C. *Organometallics* **1992**, *11*, 3712. (b) DeGrace, S. A.; Berry, S. W.; Mackie, S. C. *J. Organomet. Chem.* **1998**, *560*, 63. (c) Polowin, J.; Mackie, S. C.; Baird, M. C. *Organometallics* **1992**, *11*, 3724.

(24) Wilmes, G. M.; France, M. B.; Lynch, S. R.; Waymouth, R. M. *Organometallics* **2004**, *23*, 2405.

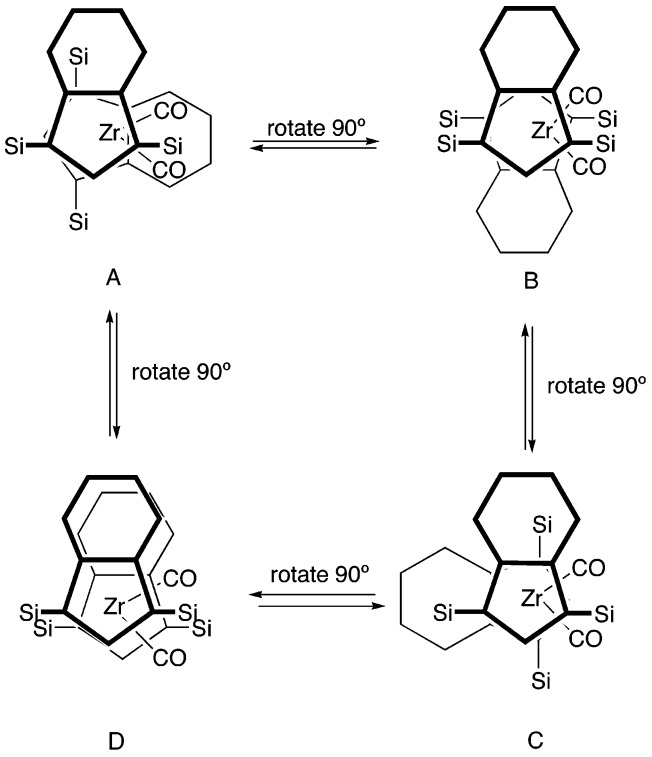

Figure 10. Gauche, eclipsed, and staggered rotamers of **1-(CO)$_2$** and **2-(CO)$_2$**. Silyl substituents are omitted for clarity.

is remarkable that slight changes in the orientational preferences of the indene ligands produce such large (~15 cm^{-1}) changes in the frequencies of the carbonyl bands. On the basis of the crystallographic data (Figure 7), we tentatively attribute the major bands to rotamer A, although a detailed computational study will be required for definitive assignment. Averaging the frequencies of the major bands observed experimentally produces a value of 1939.5 cm^{-1}, which is blue shifted 15 cm^{-1} from the corresponding cyclopentadienyl complex, (η^5-C_5H_3-1,3-($SiMe_3$)$_2$)$_2$Zr(CO)$_2$, suggesting the indenyl derivative is *electron withdrawing* relative to the Cp in this case. Thus incorporation of two silyl substituents on an indenyl anion produces a ligand with steric properties that resemble permethylcyclopentadiene but with electron-withdrawing properties that are virtually unparalleled in alkyl- or silyl-substituted Cp chemistry. The minor rotamers produce a more electron rich zirconium environment.

Similar infrared spectroscopic features are observed for **2-(CO)$_2$** and can also be rationalized by population of three vibrationally distinct rotamers in analogy to **1-(CO)$_2$**. The similarity of the frequencies for **1-(CO)$_2$** and **2-(CO)$_2$** suggests that similar rotamers are observed. Although the major isomer in **2-(CO)$_2$** displays bands at 1982 and 1902 cm^{-1}, the intensity of the minor peaks approaches those of the major. Attempts to measure perturbations to the equilibrium population as a function of temperature (22−75 °C) for **1-(CO)$_2$** by React-IR spectroscopy have been unsuccessful.

The solution IR spectrum of the most hindered member of the series, **3-(CO)$_2$**, exhibits predominantly two CO stretches, although a very minor set of additional peaks is also detectable (Figure 11). The major bands are centered at 1956 and 1874 cm^{-1}, while the

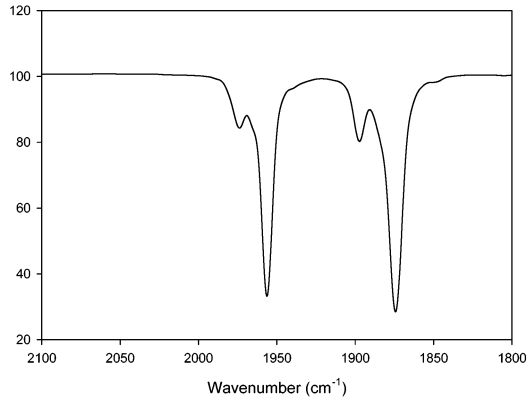

Figure 11. Pentane solution infrared spectrum of **3-(CO)$_2$**.

minor bands appear at 1976 and 1895 cm^{-1}. We attribute this difference to population of only two rotamers for this complex instead of the three observed for **1-(CO)$_2$** and **2-(CO)$_2$**. Recall that the solid state structure of **3-(CO)$_2$** exhibits an anomalous, nearly eclipsed rotamer, which contrasts the gauche arrangements observed for other crystallographically characterized tetrasubstituted zirconocene derivatives. It is also possible that other rotamers are indeed populated but have CO stretching frequencies that are not resolved by the IR experiment.

Observation of two sets of bands for the trisubstituted zirconocene dicarbonyls, **8-(CO)$_2$** and **9-(CO)$_2$**, is consistent with population of two vibrationally distinct rotamers. Only two bands are observed for **5-(CO)$_2$**, indicative of either population of one rotamer or overlapping bands. Unlike isotropic tertiary silyl and *tert*-butyl groups, the isopropyl substituents have a conformational flexibility that allows the methine hydrogens to point toward the interior of the molecule, reducing transannular interactions. As a result, the barrier for interconversion of rotamers may be reduced or population of a single rotamer becomes more significant. A similar trend was noted in the conformational energy profiles of iron piano stool complexes, where more hindered ligands resulted in higher barriers for rotation.[23]

From these data, the electronic influence of each indenyl ligand can be estimated, although absolute ordering of the ligands is difficult due to the significant differences in CO stretching frequencies observed for each rotamer. For the trisubstituted zirconocene dicarbonyls, **8-(CO)$_2$** and **9-(CO)$_2$**, comparing like bands establishes that substitution of a [CMe_3] group for a [$SiMe_3$] substituent produces a systematic red shift, demonstrating the increased electron-donating character of the [CMe_3] group. Using a similar analysis, an analogous trend can be discerned for the tetrasubstituted derivatives, **1-(CO)$_2$**, **7-(CO)$_2$**, and **4-(CO)$_2$**. Successive replacement of [$SiMe_3$] groups with [CMe_3] substituents results in progressive red shifting of the stretching frequencies. These observations may be rationalized by simple inductive effects and are supported by the Hammett σ_m values of −0.04 for [$SiMe_3$] and −0.10 for [CMe_3].[25]

The data collected in Table 3 also allow comparison of the electronic properties of the silyl substituents.

(25) Hansch, C.; Leo, A.; Taft, R. W. *Chem. Rev.* **1991**, *91*, 165.

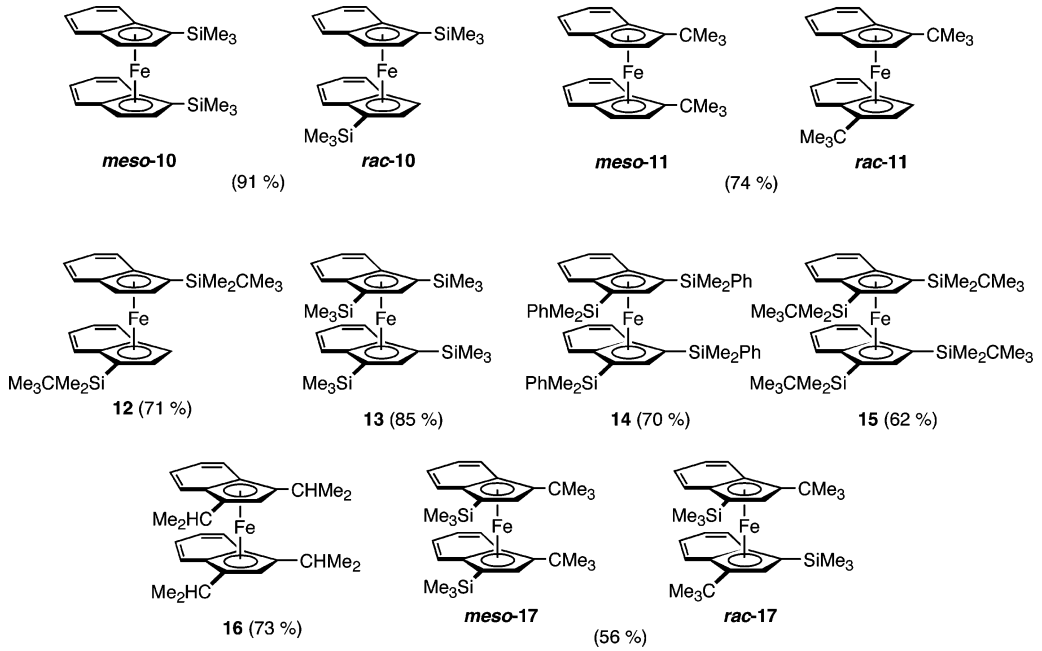

Figure 12. Labeling scheme and isolated yields of bis-indenyl iron(II) compounds.

Chart 1

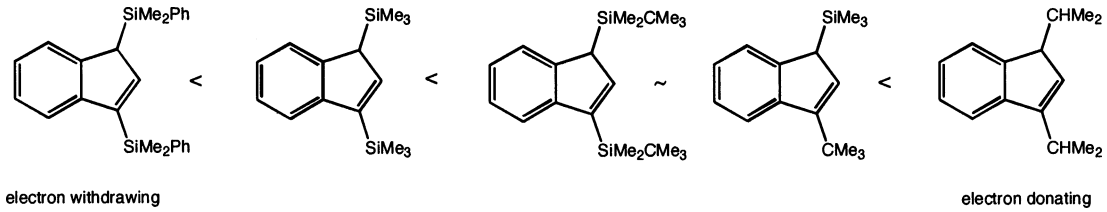

Replacing [$SiMe_3$] groups with [$SiMe_2CMe_3$] substituents results in a slight reduction of the CO stretching frequencies, indicating a small but measurable increase in electron donation in moving from **1-(CO)$_2$** to **3-(CO)$_2$**. The opposite effect is observed with [$SiMe_2Ph$], where a slight increase in carbonyl stretching frequency is observed when comparing **1-(CO)$_2$** with **2-(CO)$_2$**, demonstrating that C_9H_5-1,3-($SiMe_2Ph$)$_2$ engenders the most electrophilic zirconium center. Unfortunately, IR spectroscopy is unable to differentiate between **3-(CO)$_2$** and **4-(CO)$_2$** (Chart 1).

Preparation of Bis-indenyl Iron Complexes. Due to the complications arising from the observation of different numbers of carbonyl bands as a function of indenyl ligand, we sought an independent measure of ligand electronics. Because the preparation of biscyclopentadienyl iron(II) complexes is trivial and their reversible electrochemistry is well established, we targeted the synthesis of the corresponding series of bisindenyl iron(II) compounds. Following Wilkinson's original procedure for Ind_2Fe (Ind = η^5-C_9H_7), which calls for addition of 2 equiv of lithium indenide to an ethereal slurry of $FeCl_2$,[26] dibenzoferrocene complexes with both mono- and disubstituted indenyl ligands were prepared (Figure 12).

Both (η^5-C_9H_6-$SiMe_3$)$_2$Fe (**10**) and (η^5-C_9H_6-CMe_3)$_2$Fe (**11**) were synthesized and isolated as blue-green solids in good yields as near equimolar mixtures of diastereomers (Figure 12). Attempts to separate the diastereomers by successive recrystallizations have been unsuccessful. Incorporation of a larger [$SiMe_2CMe_3$] substituent produced only one diastereomer of **12** upon metalation with $FeCl_2$. On the basis of our current data, we are unable to definitively assign the stereochemistry, although steric arguments would suggest that the *rac* isomer should be favored.

Dibenzoferrocene derivatives containing 1,2-disubstituted indenide anions were also prepared (Figure 12). As with **10**−**12**, these molecules were isolated in good yield as blue-green, crystalline solids. For **17**, an equimolar mixture of *rac* and *meso* diastereomers were obtained and not separated. The solid state structures of both **13** and **17** were determined by X-ray diffraction and are shown in Figures 13 and 14, respectively. For **17**, only the *rac* diastereomer was observed in the lattice. Because ^{1}H NMR spectra of the crystals exhibited resonances for both the *rac* and *meso* isomers of **17**, we believe that serendipitous selection of the crystal resulted in crystallographic characterization of pure *rac*-**17**. No evidence for disorder in the structure was detected.

The angular parameters α, β, γ, and τ as well as the rotational angles have been computed for both **13** and **17** and are presented in Table 4. In both complexes, the slip distortions (ΔM−C) and fold angles (Ω) are indicative of η^5-coordinated indenyl ligands. While the fold angles for **13** and **17** are quite similar to those observed with the zirconocene dichlorides, the slip distortions are considerably smaller. The angular parameters α and β indicate a slight bending of **13** and **17** as compared to

(26) Wilkinson, G.; Pauson, P. L. *J. Am. Chem. Soc.* **1954**, *70*, 2024.

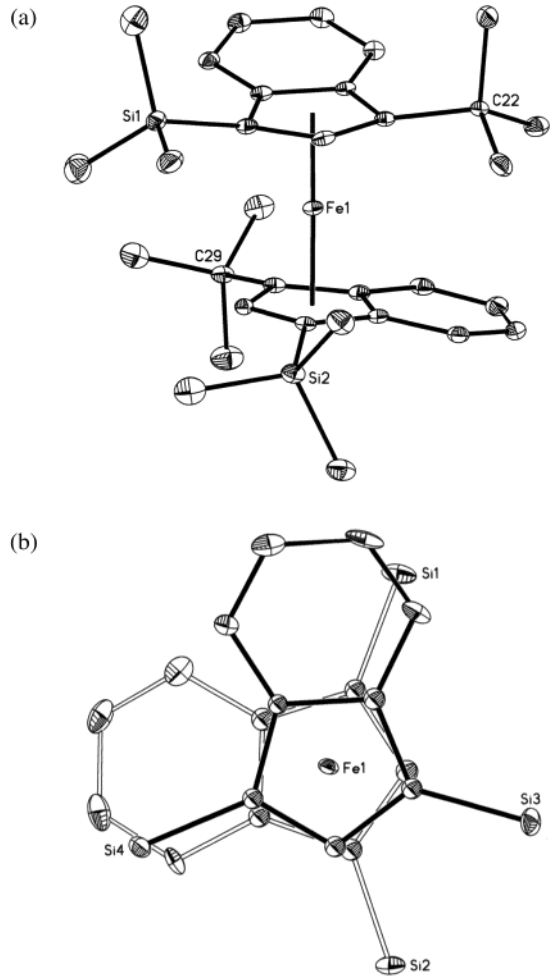

Figure 13. (a) Molecular structure of **13** with 30% probability ellipsoids. Hydrogen atoms are omitted for clarity. (b) Top view of the molecule with hydrogen atoms and silyl methyl groups omitted for clarity.

Ind_2Fe[26] or Ind^*_2Fe[27] (Table 4). In addition, the [$SiMe_3$] substituents of **13** are bent 13.5° and 16.6° out of the plane of the indenyl ligand. A similar observation is made for *rac*-**17**, where the [CMe_3] groups are displaced 15.4° and the [$SiMe_3$] groups 17.9° from the plane of the ligand. The rotational angles of 85.2(2)° and 86.7(2)°, respectively, highlight the gauche conformation in the solid state and are comparable to the zirconocene dichloride structures. All of these observations are a result of the increasing steric demand of the ligand due to the bulky [$SiMe_3$] and [CMe_3] substituents. Similar geometric preferences have been observed by Hanusa in related bis-indenyl chromium complexes[11] and by Treichel for [(η^5-C_9H_5-1,3-$(CH_3)_2$)$_2$Fe]PF_6.[27]

The solution behavior of the substituted dibenzoferrocenes was examined by variable-temperature ^{1}H NMR spectroscopy with the goal of understanding indenyl ligand conformational dynamics. At 23 °C, the ^{1}H NMR spectrum of **13** exhibits equivalent [$SiMe_3$] groups, one cyclopentadienyl hydrogen, and two distinct

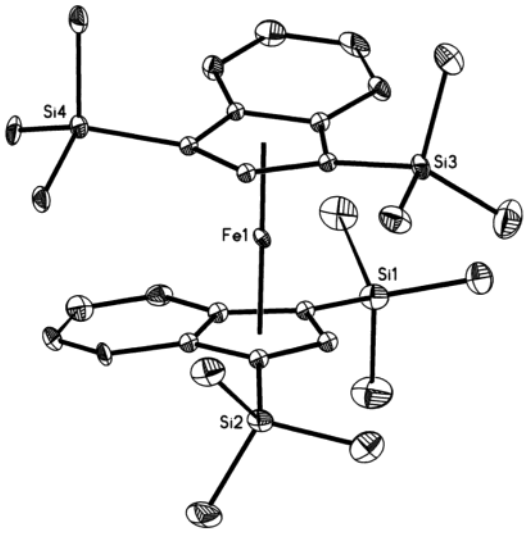

Figure 14. Molecular structure of *rac*-**14** with 30% probability ellipsoids. Hydrogen atoms are omitted for clarity.

indenyl doublets (Figure 15), suggesting a time-averaged C_{2v} symmetric metallocene arising from fast ring rotation on the time scale of the NMR experiment. Cooling the sample (T = 210 K, Figure 15) resulted in broadening of the [$SiMe_3$] and indenyl resonances, ultimately resolving into separate peaks. At 180 K, the lowest temperature accessible experimentally, near baseline resolution of the [$SiMe_3$] groups and one set of indenyl resonances is observed, suggesting restricted indenyl rotation. A similar temperature profile is observed in dichloromethane-d_2. Line shape analysis[28] was used to determine rate constants of the dynamic process, and these values were used to construct an Eyring plot (Supporting Information). As a reference value, a rate constant of 23 s^{-1} was measured at −83 °C. From these data, activation parameters of $\Delta H^{\ddagger}$ = 11.3(5) kcal/mol and $\Delta S^{\ddagger}$ = 4(2) eu were obtained for ring rotation. These values are in good agreement with activation energies of 11.0 and 15.3 kcal/mol reported for (η^5-C_5H_2-1,2,4-$(SiMe_3)_3)_2$Fe[29] and (η^5-C_5H_2-1,2,4-$(CMe_3)_3)_2$Fe,[30] respectively.

The other tetrasubstituted dibenzoferrocenes display similar ^{1}H NMR dynamics. Unfortunately, peak overlap and spectral complexity for **14** and **15** prevent a quantitative line shape analysis and extraction of activation parameters. For **14**, four resonances can be observed at 180 K for the two sets of diastereotopic methyl groups on the [$SiMe_2Ph$] substituents. On the basis of the gross features of the data, the barrier to ring rotation is on the same order of magnitude as **13**, suggesting similar steric environments imparted by each ligand.

The cyclopentadienyl region of the toluene-d_8 ^{1}H NMR spectrum of the mixture of *rac* and *meso* isomers of **17** is shown in Figure 16. At ambient temperature, the spectrum exhibits two cyclopentadienyl resonances of approximately equal area, indicative of an equimolar

Table 4. Structural Parameters for Bis-indenyl Iron(II) Complexes

compound	Δ(M−C) (Å)	Ω (deg)	RA (deg)	α (deg)	β (deg)	γ (deg)	τ (deg)
13	0.058(5), 0.066(4)	3.2(3), 3.9(4)	85.2(5)	5.8	174.2	178	1.9
rac-**17**	0.065(3), 0.065(3)	3.7(2), 3.2(2)	86.7(2)	7.2	172.8	177.3	2.25
Ind_2Fe[26]	0.054(6), 0.051(5)	2.6(4), 2.7(5)	13.0(4)	3.2	176.8	179.2	1.2
Ind^*_2Fe[34]	0.029(4)	2.4(4)	151.3(3)	0.3	179.7	179.2	−0.25

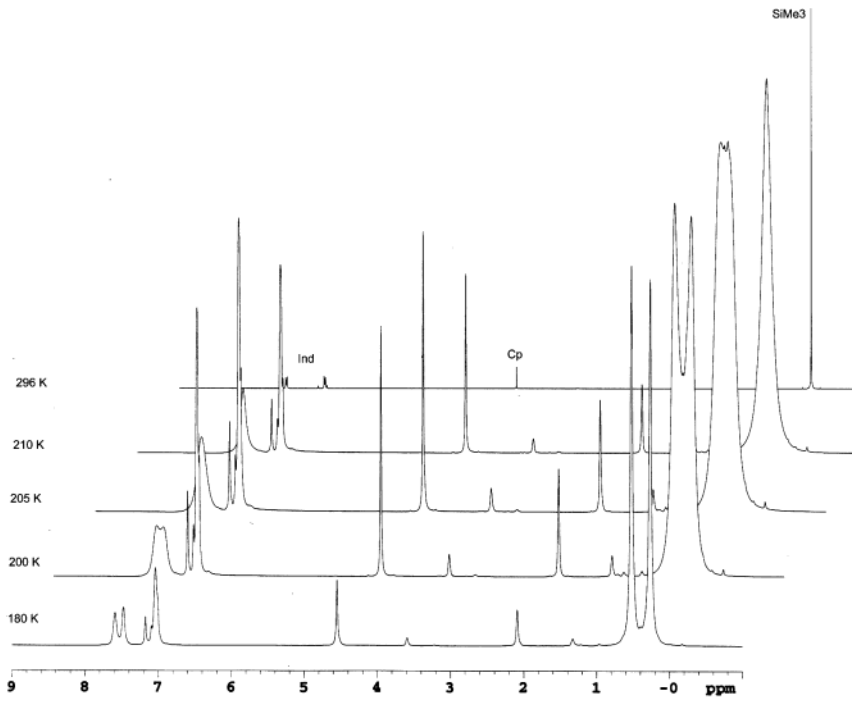

Figure 15. Variable-temperature ^{1}H NMR spectra of **13** in toluene-d_8.

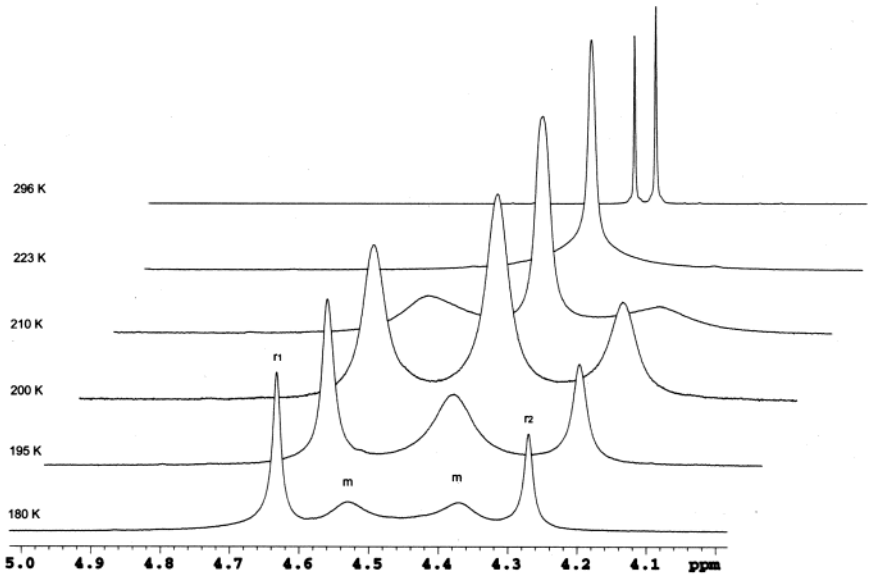

Figure 16. Cyclopentadienyl region of the ^{1}H NMR spectrum of *rac*/*meso*-**17** in toluene-d_8 as a function of temperature.

mixture of the two diastereomers in a fast exchange regime. At the lowest temperature examined, 180 K, four distinct cyclopentadienyl peaks are observed, two of which are of equal area (Figure 16). Warming the sample to 195 K resulted in coalescence of these two resonances with concomitant broadening of the remaining two peaks. The resonances coalesce at 223 K, suggesting interconversion of two rotamers on the NMR time scale. We interpret these data in terms of the model presented in Figure 17. On the basis of crystallographic data and simple steric arguments, gauche rotamers should be observed in preference to eclipsed or staggered isomers due to unfavorable interactions between the bulky [$SiMe_3$] and [CMe_3] substituents in these orientations. If only gauche rotamers are present at the static limit, *rac*-**17** would be expected to exhibit two cyclopentadienyl resonances due to the distinct rotamers A and C (Figure 17). Because of different transannular interactions, the populations of A and C could be measurably different. A similar analysis on *meso*-**17** predicts two cyclopentadienyl hydrogens in the static limit. In this case, rotamers A and C are equivalent, and therefore the two cyclopentadienyl peaks must be of equal intensity. The spectra presented in Figure 16 are consistent with this model and clearly establish restricted ring rotation at low temperatures for the two diastereomers of **17**.

(27) Treichel, P. M.; Johnson, J. W.; Calabrese, J. C. *J. Organomet. Chem.* **1975**, *88*, 215.
(28) Marat, K. *Spinworks*; University of Manitoba, 2004.
(29) Okuda, J.; Herdtweck, E. *Chem. Ber.* **1988**, *121*, 1899.
(30) Abel, E. W.; Long, N. J.; Orrell, K. G.; Osborne, A. G.; Sik, V. *J. Organomet. Chem.* **1991**, *403*, 195.

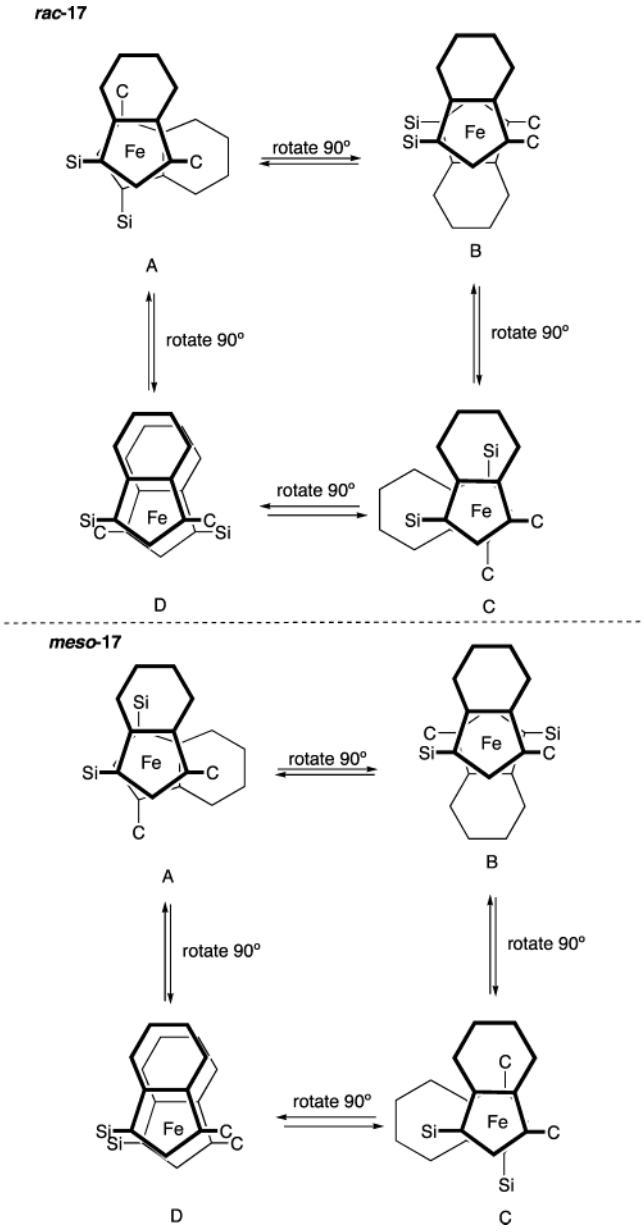

Figure 17. Rotamers of *rac*- and *meso*-**17**.

Applying the model originally developed by Okuda for [$SiMe_3$]- and [CMe_3]-substituted ferrocenes,[29,31] the conformational dynamics of the tetrasubstituted dibenzoferrocenes may be understood. Because the indenyl substituents are isotropic, we believe that the barrier of rotation arises from geared, synchronous rotations of the bulky substituents. Thus to avoid unfavorable transannular interactions, the [$SiMe_3$] groups on one indenyl ring of **13** must rotate simulataneously with the other. Similar behavior has also been observed for **14** and the mixture of *rac* and *meso* isomers of **17**.

Each of the dibenzoferrocenes reported in this study was characterized by cyclic voltammetry in 0.1 M TBAH/THF (TBAH = tetrabutylammonium hexafluorophosphate) solutions using platinum as counter and working electrodes. A silver wire was used as a quasi-reference electrode, and its potential was calibrated against ferrocene.

(31) Thornberry, M. P.; Slebodnick, C.; Deck, P. A.; Fronczek, F. R. *Organometallics* **2000**, *19*, 5352.

Table 5. Formal Potentials for a Series of Substituted Dibenzoferrocenes[a]

compound	$E_{1/2}$ (mV)
Cp_2Fe	0
10	−54
12	−71
Ind_2Fe	−85
11	−115
14	−20
13	−118
15	−122
17	−153
16	−250

[a] Reported versus ferrocene/ferrocenium.

All dibenzoferrocene derivatives examined exhibited well-behaved cyclic voltammetric responses. The voltammetric profiles are those anticipated for a freely diffusing redox couple that is chemically reversible. The peak potential difference (ΔE_p) is somewhat larger than the anticipated value of 59 mV, but this is due to ohmic losses in solution, not sluggish kinetics. This is evidenced by the fact that ferrocene itself, which is known to show rapid interfacial charge transfer kinetics, exhibited a similar response likely arising from the high resistance of the solvent.

All of the formal potentials were negatively shifted, relative to ferrocene, suggesting that every indenyl ligand is more electron donating than Cp (Table 5),[32,33] contrasting some of the results from the infrared study where disilylated indenes appeared *less* electron donating. In agreement with the carbonyl stretching frequencies, the relative electronic properties determined from electrochemistry follow the trends anticipated from inductive effects. In the series of disubstituted dibenzoferrocenes **10**−**12**, the relative electron-donating ability of the indenyl substituents is [$SiMe_3$] < [$SiMe_2CMe_3$] < [CMe_3].

A similar trend has been observed for the corresponding ferrocenes, where silyl groups are electron withdrawing and alkyl groups such as *tert*-butyl are electron donating.[34] Importantly, the formal potentials for silylated compounds **10** and **12** are shifted positive of Ind_2Fe, suggesting that the silyl groups are indeed electron withdrawing relative to hydrogen. However, as is evident from the data in Table 5, the presence of additional silyl substituents produces a shift in the formal potentials to values that are negative of dibenzoferrocene. This apparent contradiction, which suggests that the second silyl group gives rise to a net electron-donating effect, likely indicates that steric effects play a larger role than anticipated. Similar behavior has been reported by Okuda in silylated ferrocenes and was rationalized by the alleviation of unfavorable steric interactions upon oxidation to the less congested ferrocenium ion.[34] While a similar steric argument may be used here, the iron−carbon bond distances determined for **13** are within experimental error of those reported for Ind_2Fe[26] and Ind^*_2Fe.[35] However, the increased steric congestion associated with **13**, **14**, **15**, and **17** is manifested in the

(32) Treichel, P. M.; Johnson, J. W.; Wagner, K. P. *J. Organomet. Chem.* **1975**, *88*, 227.
(33) Robbins, J. L.; Edelstein, N.; Spencer, B.; Smart, J. C. *J. Am. Chem. Soc.* **1982**, *104*, 1882.
(34) Okuda, J.; Albach, R. W.; Herdtweck, E. *Polyhedron* **1991**, *10*, 1741.

Chart 2

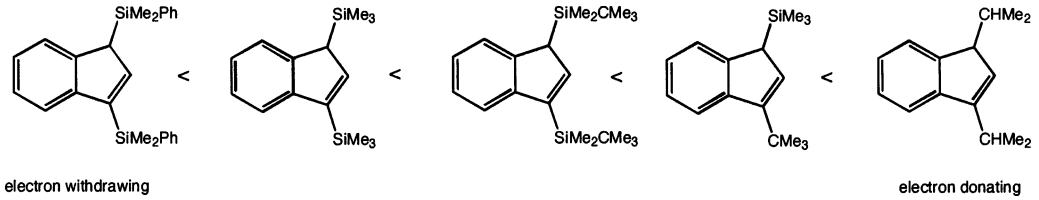

solution NMR dynamics of these molecules, where restricted ring rotation is observed at low temperature. Only time-averaged spectra consistent with rapid ring rotation are obtained for **10**−**12**. Interestingly, the formal potential for **14** is shifted to a more positive value than Ind_2Fe but not past the value for ferrocene, suggesting that the electron-donating effects overcome some of the steric effects.

The steric arguments discussed above may be used to reconcile the differences between the electrochemical and infrared spectroscopic data. From this study and that previously reported by Okuda,[34] it appears that the electrochemical experiments are more sensitive to steric effects and caution must be exercised when dealing with highly substituted cyclopentadienyl or indenyl ligands or conclusions about the absolute electronic properties of a given ligand may be tenuous. Still, we believe that the data presented in Table 5 are a reliable measure of the relative electronic properties of a given ligand set, as long as similar steric environments are maintained. Thus, whereas general comparisons among disubstituted and tetrasubstituted dibenzoferrocenes might not be as compelling, comparisons within each respective series are. Because each of the tetrasubstituted dibenzoferrocenes display similar variable-temperature NMR spectroscopic profiles, we feel confident in establishing the trend, shown in Chart 2, of the relative electron-donating properties of each disubstituted indenyl ligand. Importantly, these data are consistent with the trend established by infrared spectroscopy for the zirconocene dicarbonyl compounds.

Conclusions

The electronic properties of a family of tetrasubstituted zirconocene dicarbonyl and iron(II) sandwich complexes containing silylated and alkylated indenyl ligands have been studied by infrared spectroscopy and electrochemical experiments, respectively. Both techniques established that simple inductive effects are useful in predicting the relative electron-donating or -withdrawing capability of a ligand within a series. Pentane solution infrared spectra of highly substituted bis-indenyl zirconocenes allow observation of multiple rotamers in solution with significantly different CO stretching frequencies, the number of which depends on the size of the indenyl substituents. Special care must be taken in interpreting electrochemical data on these types of molecules, as steric effects influence the measured formal potentials. Despite these complications, the stereoelectronic properties of a family of synthetically accessible disubstituted indene ligands have been established and should provide insight into understanding the chemistry of their low-valent zirconium derivatives.

Experimental Section

General Considerations. All air- and moisture-sensitive manipulations were carried out using standard vacuum line, Schlenk, or cannula techniques or in an M. Braun inert atmosphere drybox containing an atmosphere of purified nitrogen. Solvents for air- and moisture-sensitive manipulations were initially dried and deoxygenated using literature procedures.[36] Benzene-d_6 and toluene-d_8 for NMR spectroscopy were distilled from sodium metal under an atmosphere of argon and stored over 4 Å molecular sieves or sodium metal. Dichloromethane-d_2 was distilled from CaH_2 under vacuum prior to use. Chlorotrimethylsilane was purchased from Acros Organics and dried over CaH_2 before use. Indene, Adogen-464, *tert*-butyl bromide, $SiMe_2PhCl$, $SiMe_2(CMe_3)Cl$, 1.6 M ^nBuLi in hexanes, and 1.0 M $NaBEt_3H$ in toluene were purchased from Acros and used as received. Iron(II) chloride and carbon monoxide were purchased from Aldrich. Carbon monoxide was passed through a liquid nitrogen-cooled trap before use. Preparation of the substituted indenyl ligands was carried out using standard procedures, and more specific details can be found in the Supporting Information. **1-Cl$_2$**[9] and **1-(CO)$_2$**[9] were prepared according to previously reported procedures.

^1H and ^{13}C NMR spectra were recorded on a Varian Inova 400 spectrometer operating at 399.779 MHz (^1H) and 110.524 MHz (^{13}C). Variable-temperature ^1H experiments were conducted on a Varian Inova 500 spectrometer operating at 500.62 MHz. All chemical shifts are reported relative to $SiMe_4$ using ^1H (residual) or ^{13}C NMR chemical shifts of the solvent as a secondary standard. Infrared spectroscopy was conducted on a Mattson RS-10500 Research Series FT-IR spectrometer calibrated with a polystyrene standard. Cyclic voltammograms (CVs) were collected using three-compartment electrochemical cells, with Pt working and counter electrodes and Ag wire as a reference in a drybox equipped with electrochemical outlets. CVs were recorded using a Bioanalytical Systems CV-27 voltammograph and plotted with a Soltec VP-6423S X-Y recorder. All CVs were run at a scan rate of 100 mV/s. Solutions of the individual compounds were prepared by charging 2−7 mg of the appropriate ferrocene and 0.500 g (1.3 mmol) of [n-Bu_4N][PF_6] in a vial and dissolving the solids in 13 mL of THF. This produced solutions of approximately 1 mM in ferrocene and 0.1 M in electrolyte. After recording the baseline of a standard 0.1 M solution of electrolyte, CVs were collected for each of the different ferrocenes, including Cp_2Fe. Oxidation potentials were then referenced to the formal potential of ferrocene. All compounds displayed reversible electrochemical behavior.

Single crystals suitable for X-ray diffraction were coated with polyisobutylene oil in a drybox and were quickly transferred to the goniometer head of a Siemens SMART CCD area detector system equipped with a molybdenum X-ray tube (λ = 0.71073 Å). Preliminary data revealed the crystal system. A hemisphere routine was used for data collection and determination of lattice constants. The space group was identified,

(35) Westcott, S. A.; Kakkar, A. K.; Stringer, G.; Taylor, N. J.; Marder, T. B. *J. Organomet. Chem.* **1990**, *394*, 777.

(36) Pangborn, A.; Giardello, M.; Grubbs, R. H.; Rosen, R.; Timmers, F. *Organometallics* **1996**, *15*, 1518.

and the data were processed using the Bruker SAINT program and corrected for absorption using SADABS. The structures were solved using direct methods (SHELXS) completed by subsequent Fourier synthesis and refined by full-matrix least-squares procedures. Elemental analyses were performed at Robertson Microlit Laboratories, Inc., Madison, NJ.

Preparation of 8,8-Dimethylbenzofulvene. A 500 mL round-bottomed flask was charged with 20.0 g (0.17 mol) of indene and 19.0 mL (0.26 mol) of acetone. After the liquids were diluted in approximately 150 mL of MeOH, 21.0 mL (0.25 mol) of pyrollidine was added. The reaction mixture was stirred for 24 h at room temperature. The excess pyrollidine was then quenched with 21 mL (0.25 mol) of concentrated acetic acid. Water (300 mL) was added, and the product was extracted four times with 250 mL portions of diethyl ether. The resulting diethyl ether layer was collected and washed twice with 300 mL portions of water and then dried over $MgSO_4$. Filtration followed by solvent removal in vacuo afforded 18.5 g (68%) of 8,8-dimethylbenzofulvene, which was used without additional purification. ^{1}H NMR (benzene-d_6): δ 1.74 (s, 3H, Me), 1.88 (s, 3H, Me), 6.63 (s, 2H, Cp), 7.08 (m, 2H, Ind), 7.20 (d, 9 Hz, 1H, Ind), 7.56 (d, 9 Hz, 1H, Ind). ^{13}C NMR (benzene-d_6): δ = 50.79 (Me), 54.61 (Me), 121.38, 123.89, 125.01 (Cp), 126.35, 128.82, 136.40, 137.42, 142.33, 144.60 (Ind). One resonance not located.

Preparation of 3-Isopropylindene. In a drybox, a 500 mL three-necked flask was charged with 5.33 g (0.14 mol) of $LiAlH_4$. Against an Ar counterflow, 150 mL of diethyl ether was added by cannula. Through an addition funnel, a 150 mL of a diethyl ether solution containing 18.5 g (0.12 mol) of 8,8-dimethylbenzofulvene was added dropwise over the course of 1 h. The reaction was stirred for an additional 8 h, after which time approximately 20 mL of a 15% aqueous NaOH solution was then carefully added over the course of 1 h or until the evolution of dihydrogen was complete. **Caution: The reaction is highly exothermic and produces large amounts of H_2(g)!** Approximately 200 mL of H_2O was then added to the reaction mixture, and the product was extracted with three 300 mL portions of diethyl ether. The organic layer was collected and washed with two 300 mL portions of water and then dried over $MgSO_4$. Filtration followed by solvent removal in vacuo afforded 16.0 g (85%) of a red oil identified as 3-isopropylindene, which was used without further purification. ^{1}H NMR (benzene-d_6): δ 1.12 (d, 9 Hz, 6H, CH(CH_3)$_2$), 2.70 (s, 9 Hz, 1H, CH(CH$_3$)$_2$), 2.96 (s, 2H, CH_2), 5.88 (s, 1H, Cp), 7.07 (m, 2H, Ind), 7.14 (d, 9 Hz, 1H, Ind), 7.24 (d, 9 Hz, 1H, Ind).

Preparation of 3-Isopropyl-8,8-dimethylbenzofulvene. A 1 L round-bottomed flask was charged with 16.0 g (0.11 mol) of 3-isopropylindene and 10.0 g (0.18 mol) of crushed KOH pellets. A reflux condenser was attached, and approximately 150 mL of DME was added. The resulting reaction mixture was heated to reflux, and 16 mL (0.22 mmol) of acetone was added. The reaction mixture was then heated for an additional 12 h, forming a purple solution. After cooling to room temperature, approximately 300 mL of H_2O was added, and a workup similar to that described for 8,8-dimethylbenzofulvene was performed. This procedure yielded 19.0 g (86%) of a red oil identified as 3-isopropyl-8,8-dimethylbenzofulvene, which was used without further purification. ^{1}H NMR (benzene-d_6): δ 1.25 (d, 8 Hz, 6H, CH(CH_3)$_2$), 1.90 (s, 3H, Me), 2.03 (s, 3H, Me), 2.88 (s, 9 Hz, 1H, CH(CH$_3$)$_2$), 6.57 (s, 1H, Cp), 7.21 (m, 2H, Ind), 7.31 (d, 8 Hz, 1H, Ind), 7.69 (d, 8 Hz, 1H, Ind). ^{13}C NMR (benzene-d_6): δ 22.22, 22.46, 24.44, 26.99 (CH_3 and CHMe_2), 28.07 (CH(CH$_3$)$_2$), 119.41, 120.86, 123.90 (Cp), 124.99, 126.03, 136.48, 137.64, 139.11, 144.21, 148.59 (Ind).

Preparation of 1,3-Diisopropylindene. A 250 mL round-bottomed flask was charged with 5.0 g (25 mmol) of 3-isopropyl-8,8-dimethylbenzofulvene and approximately 100 mL of diethyl ether. To the resulting red solution, 27.5 mL (28 mmol) of a 1.0 M solution of $NaBEt_3H$ in toluene was added, and the reaction mixture was stirred for 3 h. Once complete, the flask was transferred outside of the drybox, and approximately 100 mL of H_2O was added to quench any excess $NaBEt_3H$. A workup procedure similar to that described for 8,8-dimethylbenzofulvene was followed. Vacuum distillation afforded 3.1 g (65%) of 1,3-diisopropylindene suitable for deprotonation. ^{1}H NMR (benzene-d_6): δ 0.60 (d, 10 Hz, 3H, CH(CH_3)$_2$), 0.99 (d, 10 Hz, 3H, CH(CH_3)$_2$), 1.21 (m, 6H, CH(CH_3)$_2$), 2.17 (m, 1H, CH(CH$_3$)$_2$), 2.78 (m, 1H, CH(CH$_3$)$_2$), 3.24 (br s, 1H, Cp), 6.05 (s, 1H, Cp), 7.26 (m, 4H, Ind). ^{13}C NMR (benzene-d_6): δ 17.54, 21.62, 21.98, 22.19, 27.21, 30.36 (CHMe_2), 55.32, 119.644, 123.33 (Cp), 124.90, 126.54, 145.33, 148.22, 151.35 (Ind). One indene resonance not located.

Preparation of (η^5-C_9H_5-1,3-(SiMe$_2$Ph)$_2$)$_2$ZrCl$_2$ (2-Cl$_2$). A 500 mL round-bottomed flask was charged with 3.24 g (8.30 mmol) of Li[C_9H_5-1,3-(SiMe$_2$Ph)$_2$] and approximately 150 mL of diethyl ether. The resulting yellow solution was chilled in a cold well cooled to liquid nitrogen temperature, and 0.969 g (4.16 mmol) of $ZrCl_4$ was added. The reaction mixture was stirred for 1 day, and the solvent was removed in vacuo. The resulting solid was dissolved in dichloromethane and filtered through a pad of Celite. Removal of dichloromethane in vacuo yielded a brown oil that was recrystallized from diethyl ether at −35 °C to afford 2.58 g (67%) of **2-Cl$_2$** as a yellow solid. Anal. Calcd for $C_{50}H_{54}Si_4ZrCl_2$: C, 64.61; H, 5.86. Found: C, 64.37; H, 5.45. ^{1}H NMR (benzene-d_6): δ 0.69 (s, 12H, SiMe_2Ph), 0.75 (s, 12H, SiMe_2Ph), 6.84 (m, 4H, Ind), 7.23 (s, 2H, Cp), 7.25 (m, 20H, Ph), 7.60 (m, 4H, Ind). ^{13}C NMR (benzene-d_6): δ −0.37 (SiMe_2Ph), −0.02 (SiMe_2Ph), 119.89, 126.43 (Cp), 128.05, 128.39, 129.27, 134.09, 136.45, 138.34, 139.42 (Ind/Ph).

Preparation of [(η^5-C_9H_5-1,3-(SiMe$_3$)$_2$)ZrCl$_3$·(Et$_2$O)$_2$·LiCl$_x$]$_n$. A 100 mL round-bottomed flask was charged with 0.931 g (4.00 mmol) of $ZrCl_4$, and approximately 50 mL of diethyl ether was added. The slurry was chilled in a cold well cooled to liquid nitrogen temperature for an additional 15 min. The flask was removed from the cold well, and 1.07 g (3.98 mmol) of Li[C_9H_5-1,3-(SiMe$_3$)$_2$] was then added in small portions over the course of several minutes. The reaction mixture was allowed to warm to ambient temperature and stirred overnight. The resulting orange-yellow solution was filtered through Celite, and the solvent was removed in vacuo to yield 2.02 g (91%) of an oily orange-yellow solid identified as [(η^5-C_9H_5-1,3-(SiMe$_3$)$_2$)ZrCl$_3$·(Et$_2$O)$_2$·LiCl$_x$]. ^{1}H NMR (benzene-d_6): δ 0.44 (s, 18H, SiMe_3), 1.04 (br s, 12H, CH_3CH$_2$O), 3.24 (br s, 8H, CH$_3$CH_2O), 7.05 (br s, 2H, Ind), 7.38 (s, 1H, Cp), 7.79 (m, 2H, Ind). ^{13}C NMR (benzene-d_6): δ 0.41 (SiMe_3), 15.06 (CH_3CH$_2$O), 65.98 (CH$_3$$CH_2$O), 121.42, 126.15 (Cp), 126.57, 136.64, 138.22 (Ind).

Preparation of (η^5-C_9H_5-1,3-(SiMe$_3$)$_2$)(η^5-C_9H_5-1,3-(SiMe$_2$Ph)$_2$)ZrCl$_2$ (6-Cl$_2$). In a 100 mL round-bottomed flask, 6.62 mmol of [(η^5-C_9H_5-1,3-(SiMe$_3$)$_2$)ZrCl$_3$·(Et$_2$O)$_2$·LiCl$_x$] was generated in situ, and the resulting diethyl ether slurry was chilled in a liquid nitrogen cooled cold well for 30 min. The flask was removed, 2.59 g (6.63 mmol) of Li[C_9H_5-1,3-(SiMe$_2$Ph)$_2$] was added to the mixture, and the reaction was stirred overnight. The solvent was removed in vacuo, the resulting yellow solid was extracted into dichloromethane, and the solution was filtered through Celite. Removal of the solvent in vacuo and recrystallization of the resulting yellow solid from diethyl ether at −35 °C afforded 2.24 g (42%) of **6-Cl$_2$**. Anal. Calcd for $C_{40}H_{50}Si_4ZrCl_2$: C, 59.66; H, 6.26. Found: C, 59.94; H, 5.87. ^{1}H NMR (benzene-d_6): δ 0.29 (s, 18H, SiMe_3), 0.73 (s, 6H, SiMe_2Ph), 0.77 (s, 6H, SiMe_2Ph), 6.80 (m, 2H, Ind), 6.98 (m, 2H, Ind), 7.00 (s, 1H, Cp), 7.10 (m, 3H, Cp/Ph), 7.15 (m, 4H, Ph), 7.22 (m, 4H, Ph), 7.62 (m, 2H, Ind), 7.67 (m, 2H, Ind). ^{13}C NMR (benzene-d_6): δ −0.31 (SiMe_2Ph), 0.24 (SiMe_2Ph), 1.14 (SiMe_3), 119.66, 121.84, 126.24, 126.37 (Cp), 129.28, 134.13, 135.57, 138.07, 138.48, 139.47 (Ind/Ph). Four Ind/Ph resonances not located.

Preparation of (η^5-C_9H_5-1,3-($SiMe_3$)$_2$)(η^5-C_9H_6-$SiMe_3$)Zr-(CO)$_2$ (8-(CO)$_2$). A thick walled glass bomb was charged with 0.275 g (0.45 mmol) of **8-Cl$_2$** and 0.115 g (4.7 mmol) of activated Mg turnings. On a vacuum line, approximately 15 mL of THF was vacuum transferred onto the solids and the resulting slurry frozen in liquid nitrogen. One atmosphere of CO was added to the vessel at −196 °C. The vessel was thawed by warming to room temperature and then placed in a 45 °C oil bath for 18 h. The CO atmosphere and the solvent were then removed in vacuo, leaving a green residue. The vessel was taken into the drybox and the residue extracted into pentane. Filtration through Celite followed by solvent removal and recrystallization from pentane at −35 °C afforded 0.142 g (53%) of **8-(CO)$_2$** as a forest green solid. Anal. Calcd for $C_{29}H_{38}Si_3ZrO_2$: C, 58.63; H, 6.45. Found: C, 57.95; H, 6.52. ^{1}H NMR (benzene-d_6): δ 0.20 (s, 9H, SiMe_3), 0.28 (s, 9H, SiMe_3), 0.31 (s, 9H, SiMe_3), 4.29 (d, 5 Hz, 1H, Cp), 5.19 (s, 1H, Cp), 5.92 (d, 5 Hz, 1H, Cp), 6.78 (m, 2H, Ind), 6.82 (m, 1H, Ind), 6.87 (m, 2H, Ind), 7.21 (m, 1H, Ind), 7.29 (m, 1H, Ind), 7.33 (d, 10 Hz, 1H, Ind). ^{13}C NMR (benzene-d_6): δ 0.01 (SiMe_3), 0.36 (SiMe_3), 0.48 (SiMe_3), 89.98, 95.19, 95.97, 96.41, 101.23, 106.07 (Cp), 121.31, 122.56, 123.27, 123.49, 123.75, 124.14, 124.54, 125.85, 126.17, 126.50, 127.19, 127.90 (Ind), 260.42 (Zr-*C*O), 264.04 (Zr-*C*O).

Preparation of *rac/meso*-(η^5-C_9H_6-($SiMe_3$))$_2$Fe (10). A 20 mL scintillation vial was charged with 0.076 g (0.60 mmol) of $FeCl_2$ and approximately 5 mL of diethyl ether. The resulting slurry was chilled to −35 °C in the drybox freezer, after which time 0.233 g (1.20 mmol) of Li[C_9H_6-($SiMe_3$)] was added as an ethereal solution over the course of 5 min. The reaction mixture was stirred for 3 h and then filtered through a pad of Celite. The diethyl ether was removed in vacuo and the resulting solid recrystallized from diethyl ether at −35 °C, affording 0.234 g (91%) of a blue-green solid identified as **10** as an equimolar mixture of *rac* and *meso* isomers. Anal. Calcd for $C_{24}H_{30}Si_2Fe$: C, 66.95; H, 7.02. Found C, 67.22; H, 6.77. ^{1}H NMR (benzene-d_6): δ 0.40 (s, 18H, SiMe_3), 0.45 (s, 18H, SiMe_3), 3.28 (br s, 1H, Cp), 3.93 (br s, 1H, Cp), 4.63 (br s, 1H, Cp), 4.88 (br s, 1H, Cp), 6.50 (t, 4 Hz, 2H, Ind), 6.74 (m, 4H, Ind), 6.8−7.0 (m, 6H, Ind), 7.51 (d, 8 Hz, 2H, Ind), 7.59 (d, 8 Hz 2H, Ind). ^{13}C NMR (benzene-d_6): δ 0.56 (SiMe_3), 0.64 (SiMe_3), 61.83, 65.39, 65.80, 74.27, 78.25, 90.13 (Cp), 90.38, 90.60, 122.39, 122.57, 122.72, 124.15, 124.49, 124.57, 126.47, 127.22, 129.95, 130.77 (Ind).

Acknowledgment. We would like to thank the Cornell University Department of Chemistry and Chemical Biology, the donors of the Petroleum Research Fund administered by the American Chemical Society, and the National Science Foundation (predoctoral fellowship to C.A.B. and CAREER Award to P.J.C.) for generous financial support. P.J.C. is also a Cottrell Scholar and would like to acknowledge financial support from the Research Corporation. We also thank Mark Wall and David Bray of the MIT Department of Chemistry Instrument Facility for access to spectrometer time.

Supporting Information Available: Additional experimental details for the preparation of indenyl ligands,[37] zirconocene dichloride, and dicarbonyl complexes as well as dibenzoferrocene derivatives. Crystallographic data for **1-Cl$_2$**, **2-Cl$_2$**, **7-Cl$_2$**, **9-Cl$_2$**, **3-(CO)$_2$**, **13**, and *rac*-**17** including full atom labeling schemes and complete bond distances and angles. Representative infrared spectra recorded in KBr, variable-temperature NMR data, and Eyring plot for **13**. This material is available free of charge via the Internet at http://pubs.acs.org.

OM0495675

(37) (a) Resconi, L.; Balboni, C.; Baruzzi, G.; Flori, C.; Guidotti, S.; Mercandelli, P.; Sirioni, A. *Organometallics* **2000**, *19*, 420. (b) Davison, A.; Rakita, P. E. *J. Organomet. Chem.* **1970**, *23*, 407.